# Tuning the efficiency and product composition for electrocatalytic $CO_2$ reduction to syngas over zinc films by morphology and wettability

Pengsong Li[a,b], Jiyuan Liu[a,b], Jiahui Bi[a,b], Qinggong Zhu[a,b,*], Tianbin Wu[a], Jun Ma[a], Farao Zhang[c], Jinchao Jia[c], and Buxing Han[a,b,d,*]

[a]Beijing National Laboratory for Molecular Sciences, CAS Key Laboratory of Colloid, Interface and Chemical Thermodynamics, CAS Research/Education Center for Excellence in Molecular Sciences, Institute of Chemistry, Chinese Academy of Sciences, Beijing,100190, China;

[b]University of Chinese Academy of Sciences; Beijing 100049, China

[c]Ningbo MaterChem Technology Co. Ltd., Ningbo, 315830, China

[d]Shanghai Key Laboratory of Green Chemistry and Chemical Processes, School of Chemistry and Molecular Engineering, East China Normal University Shanghai, 200062, China

* To whom correspondence should be addressed. E-mail: hanbx@iccas.ac.cn; qgzhu@iccas.ac.cn.

## Experimental Section

### Materials.

Zn foil (99.99%, 0.25 mm), $ZnSO_4 \cdot 7H_2O$ (>99%), zinc acetate dihydrate (>98%) and $(NH_4)_2SO_4$ (99.95%) were purchased from Alfa Aesar China Co., Ltd. ZnO (99.999%), KOH (99.99%) and hexadecyl trimethyl ammonium bromide (CTAB, 99.99%) were obtained from Sigma-Aldrich. Polytetrafluoroethylene (PTFE, 60 wt.%) and $KHCO_3$ (>99.99% metals basis) were provided by Aladdin. $CO_2$ (Beijing Beiwen Gas Chemical Industry Co., Ltd., research grade) had a purity of 99.999 % and used as received. Nafion N-117 membrane (0.180 mm thick, ≥0.90 meg/g exchange capacity) was purchased from Alfa Aesar China Co., Ltd. All chemicals used as received. Aqueous solutions were prepared with deionized water (Millipore 18.2 MΩ cm).

### Synthesis of Zn film electrodes.

***Zn-1 (Zn leaf film).*** Zn foil was prepared by mechanical polishing using SiC sandpaper (200 grit), followed by sonication in water and ethanol for 5 min. Saturated calomel electrode (SCE) and Pt gauze were used as reference electrode and counter electrode, respectively. The precursor electrolyte was an aqueous solution of 0.1 M $ZnSO_4 \cdot 7H_2O$ and 1.5 M $(NH_4)_2SO_4$. Zn-1 was fabricated in the three-electrode system with Zn foil as the working electrode at two potentials of -1.5 and -2.0 V vs. SCE. Each potential was kept for 3 s with a total of 30 repetitions. The resulting Zn-1 electrode was withdrawn and rinsed thoroughly with distilled water.

***Zn-2 (Zn wire film).*** 25 mmol ZnO powder was dissolved in 6M KOH solution to form the precursor electrolyte for Zn-2 deposition. SCE and Pt gauze were used as reference electrode and counter electrode, respectively. Zn-2 was fabricated at the potential of -1.6 V vs. SCE with Zn foil as the working electrode for 200s.

***Zn-3 (Zn sheet film).*** The precursor electrolyte was an aqueous solution of 100 g $L^{-1}$ Zn acetate dihydrate with 1 mM CTAB. SCE and Pt gauze were used as reference electrode and counter electrode, respectively. Zn-3 was fabricated at two potentials of -1.5 and -2.0 V vs. SCE with Zn foil as the working electrode. Each potential was kept for 3 s with a total of 100 repetitions.

### Preparation of aerophilic Zn electrode

To coat PTFE on the Zn surface, the as-prepared Zn electrode was soaked in PTFE dispersion (0.1 wt.%, 0.2 wt.%, 0.3 wt.%, 0.4 wt.%, and 0.5 wt.%) for 10 min, then annealed at 350 °C for 30 min under an air atmosphere. The subsequent reducing procedure was conducted at the potential of -1.5 V vs. Ag/AgCl in 0.5 M $KHCO_3$ with saturated $CO_2$ for 10 min. The 0.3 wt.% PTFE modified electrodes are denoted as Zn-1P, Zn-2P and Zn-3P, respectively. As comparison, pristine Zn electrodes (Zn-1, Zn-2 and Zn-3) were made following the same procedures but without coating with PTFE.

### Structural characterizations

The morphologies of materials were characterized by a HITACHI S-4800

scanning electron microscope (SEM) and a JEOL JEM-2100F high-resolution transmission electron microscopy (HR-TEM). Powder X-ray diffraction (XRD) patterns were acquired with an X-ray diffractometer (Model D/MAX2500, Rigaka) with Cu-Kα radiation, and the scan speed was 5°/min. The Quasi in situ X-ray photoelectron spectra (XPS) were measured on an AXIS ULTRA DLD spectrometer with Al $K_\alpha$ resource (*hv* = 1486.6 eV). The samples were prepared in a glove box and transferred to the XPS chamber for the measurement. The static contact angles were measured using an OCA20 apparatus (Data-Physics, Germany) and 10 uL water droplets.

**Electrochemical measurements**

An electrochemical workstation (CHI 660E, Shanghai CH Instruments Co., China) was used for the electrochemical experiment. The electrolysis experiments were conducted in a typical H-type cell. The as synthesized electrodes were used as the working electrodes. The Ag/AgCl (saturated KCl) electrode was used as the reference electrode and the Pt gauze was used as counter electrode. The cathode and anode compartments were separated through the Nafion 117 proton exchange membrane. 0.5 M $KHCO_3$ aqueous solution was used as the electrolyte. Under the continuous stirring, $CO_2$ was bubbled into the catholyte for 30 min before electrolysis. After that, electrochemical $CO_2$ reduction was carried out with continuous $CO_2$ bubbling (20 mL/min). The gaseous product of electrochemical experiments was collected by using a gas bag and analyzed by gas chromatography (GC, HP 4890D).

**Electrochemical impedance spectroscopy (EIS) measurement**

The EIS measurement was conducted in 0.5 M $KHCO_3$ electrolyte with saturated $CO_2$ at the potential of -1.3 V vs. Ag/AgCl with an amplitude of 5 mV of 0.1 to $10^4$ Hz.

**Electrochemical surface area (ECSA) measurement**

The cyclic voltammetry measurement was conducted in 0.5 M $KHCO_3$ electrolyte with saturated $CO_2$ using a three-electrode system, and the as-prepared electrode as the working cathode. Cyclic voltammetric measurements of the catalysts were conducted from -1.05 to -1.1 V vs. Ag/AgCl with various scan rates to obtain the double layer capacitance ($C_{dl}$) of different catalysts. The $C_{dl}$ was estimated by plotting the Δj (ja-jc) at -1.075 V vs. Ag/AgCl against the scan rates, in which ja and jc were the anodic and cathodic current densities, respectively. The linear slope was equivalent to twice of the $C_{dl}$.

## Supplementary Figures

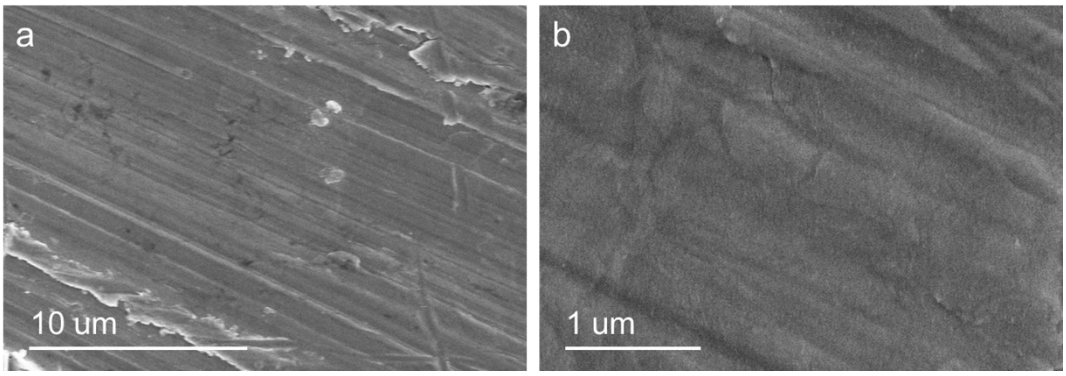


**Figure S1.** SEM images of Zn foil substrate.

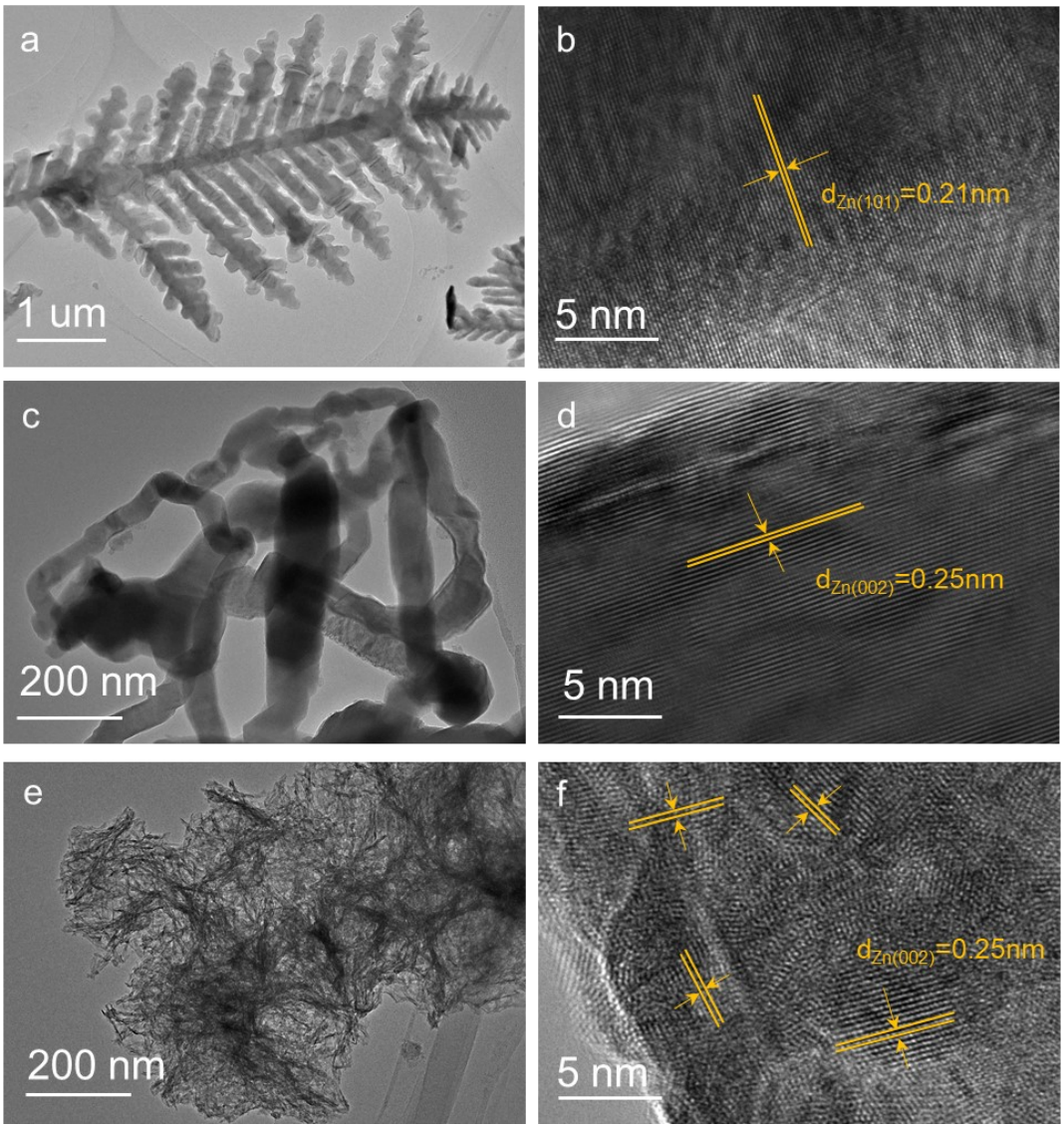


**Figure S2.** TEM and HRTEM images of (a, b) Zn-1,(c, d) Zn-2, and (e, f) Zn-3.

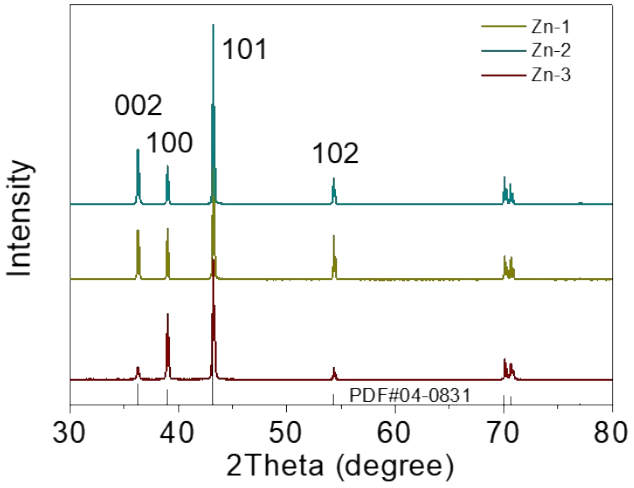


**Figure S3.** XRD patterns of Zn-1, Zn-2, and Zn-3.

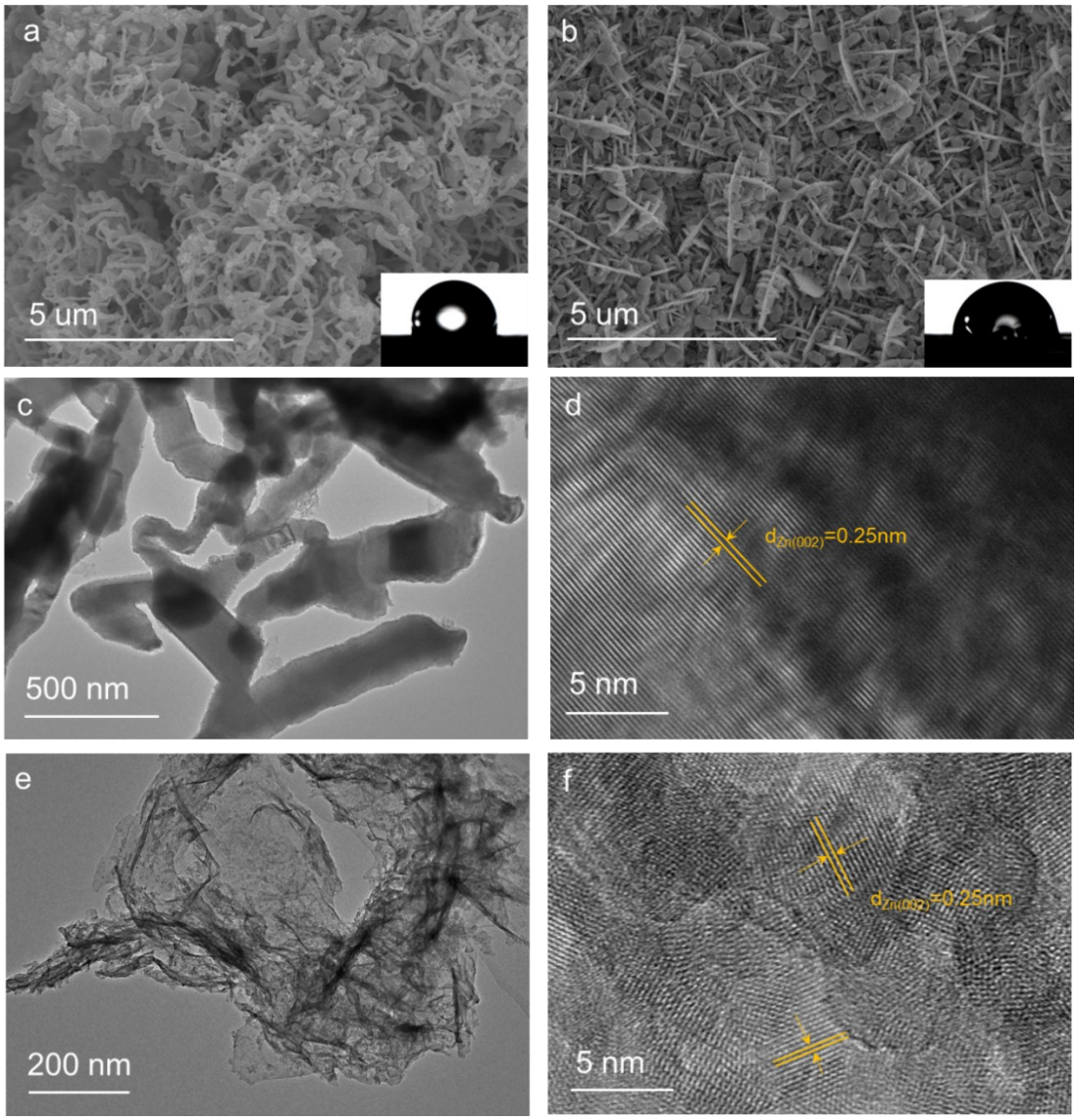


**Figure S4.** (a, b) SEM, (c, e) TEM, and (d, f) HR-TEM images of Zn-2 and Zn-3 after 0.3 wt.% PTFE modification. Insets in (a, b) show photographs of water contact angle on each electrode.

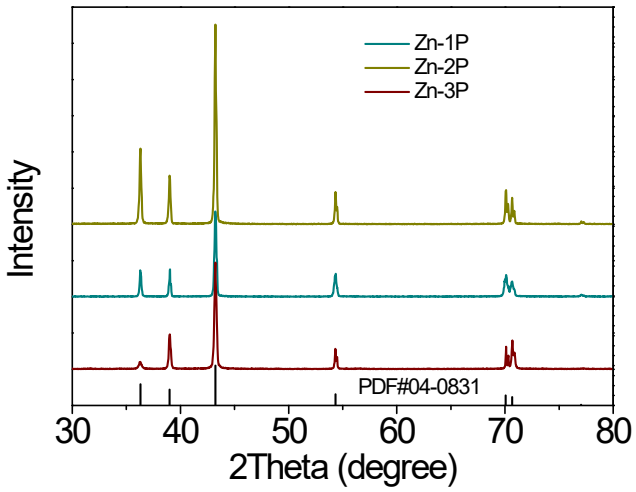


**Figure S5.** XRD patterns of Zn-1, Zn-2 and Zn-3 after 0.3 wt.% PTFE modification.

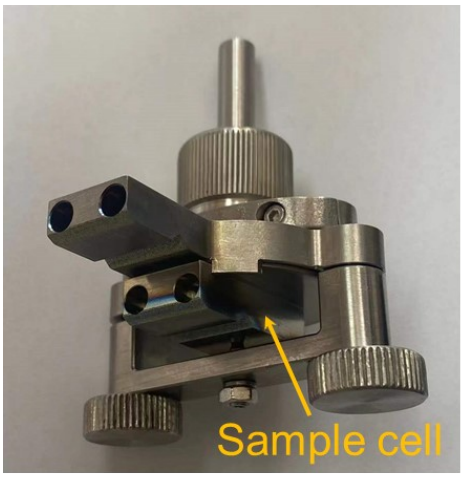


**Figure S6.** The quasi-operando XPS cell used in this work.

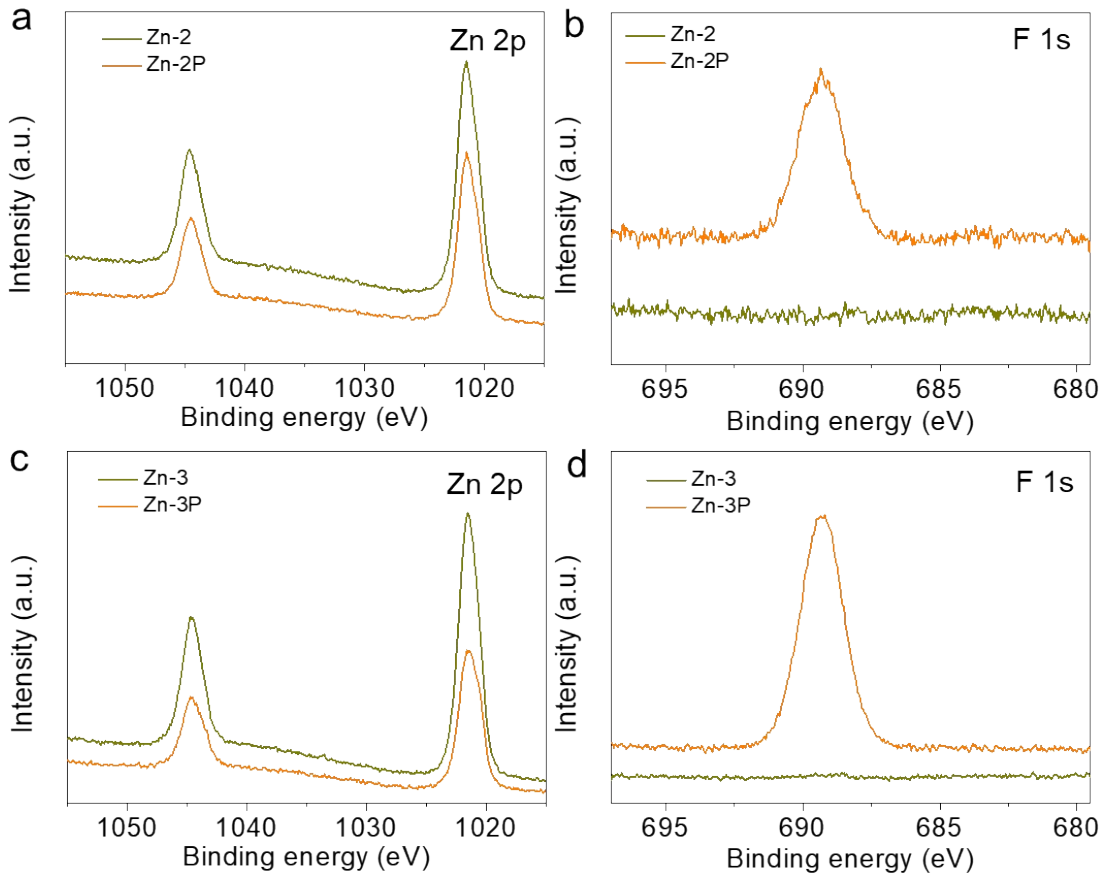


**Figure S7.** Quasi-in situ XPS spectra of Zn 2p and F 1s in the Zn-2 and Zn-3 before and after 0.3 wt.% PTFE modification.

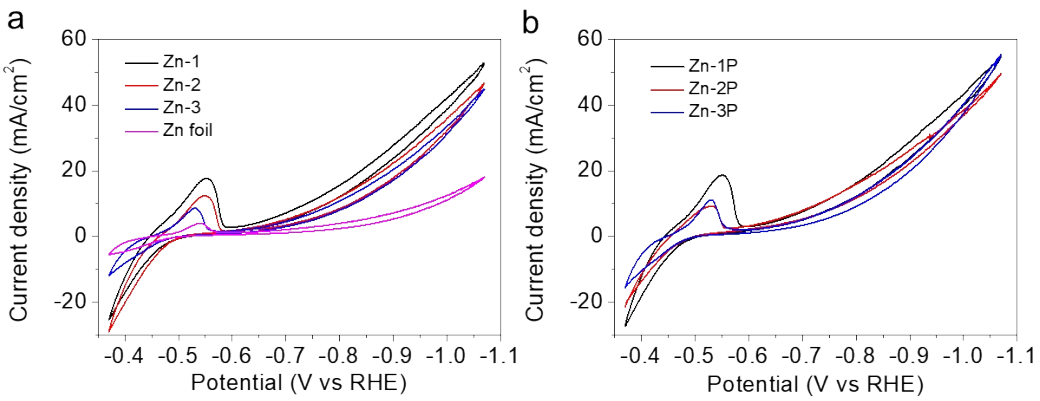


**Figure S8.** Cyclic voltammetry (CV) measurements over Zn film electrodes before and after 0.3 wt.% PTFE modification in $CO_2$-saturated 0.5 M $KHCO_3$ with the scan rate of 50 mV/s.

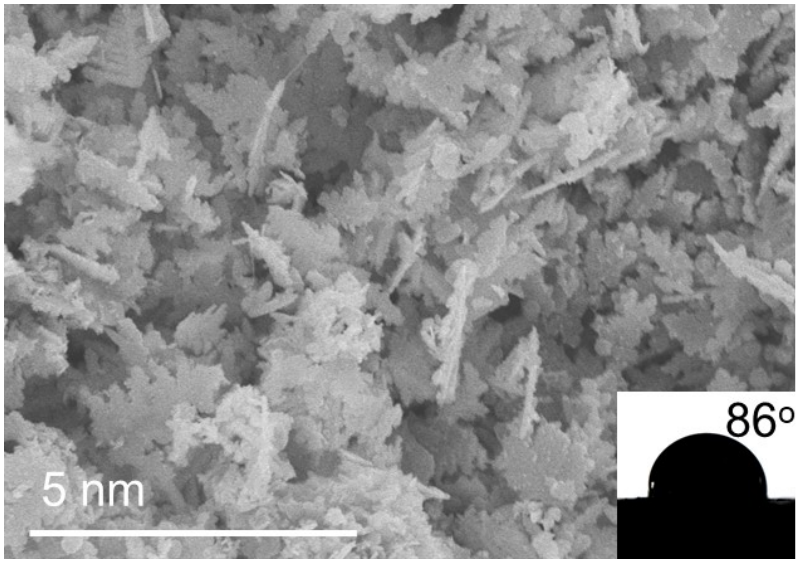


**Figure S9.** SEM image and water contact angle of 0.3 wt.% PTFE modified Zn-1 after 12 h electrocatalysis in $CO_2$-saturated 0.5 M $KHCO_3$ electrolyte at the potential of -0.97 V vs. RHE.

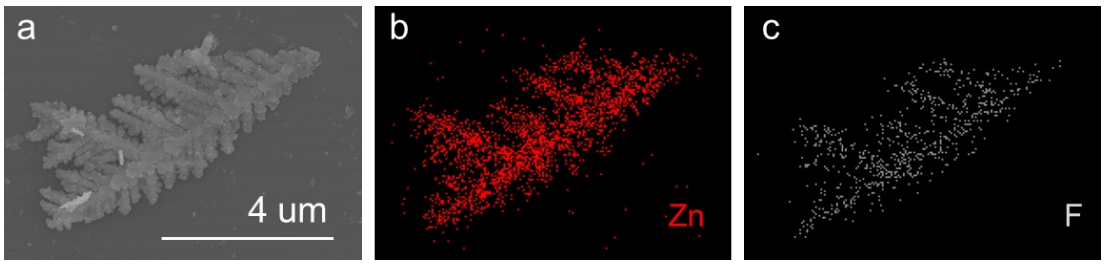


**Figure S10.** SEM (a) and corresponding element mapping (b, c) images of 0.3 wt.% PTFE modified Zn-1 after 12 h electrocatalysis in $CO_2$-saturated 0.5 M $KHCO_3$ electrolyte at the potential of -0.97 V vs. RHE.

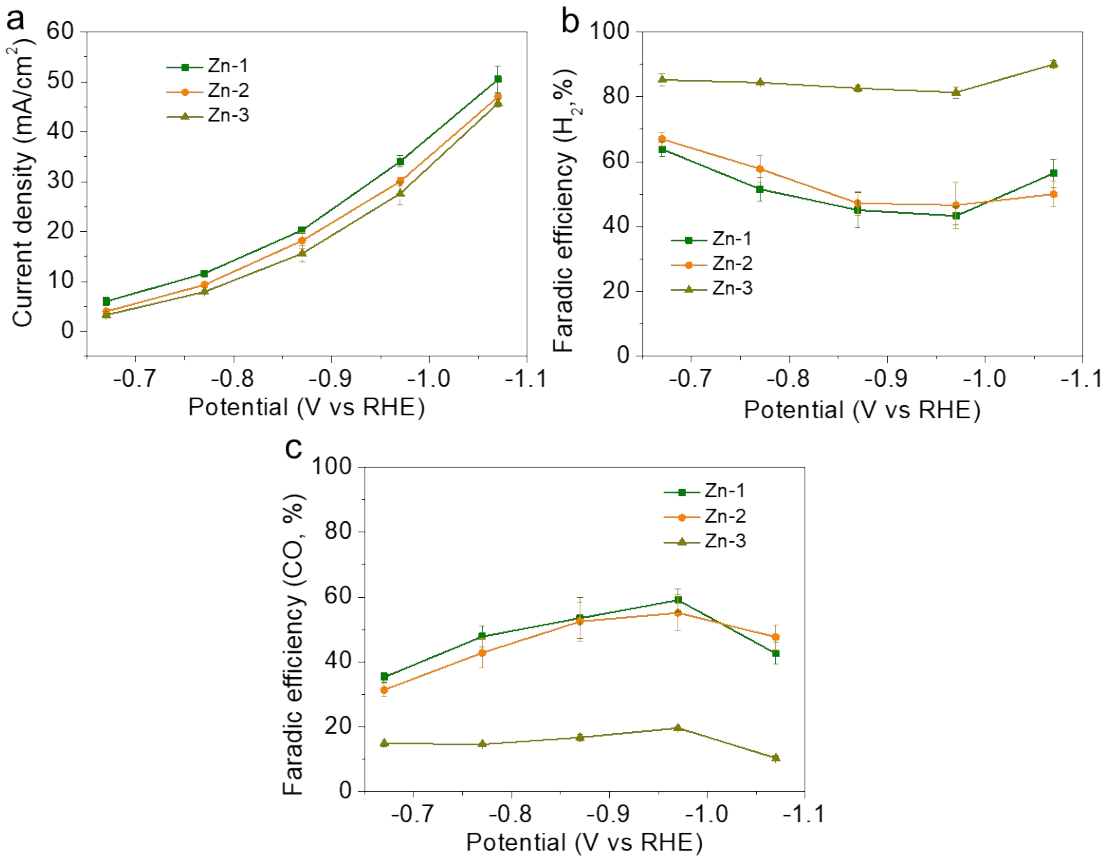


**Figure S11.** (a) Current density, (b) FE of $H_2$, and (c) FE of CO products over Zn-1, Zn-2, and Zn-3. Error bars represent the standard deviation of multiple independent experiments.

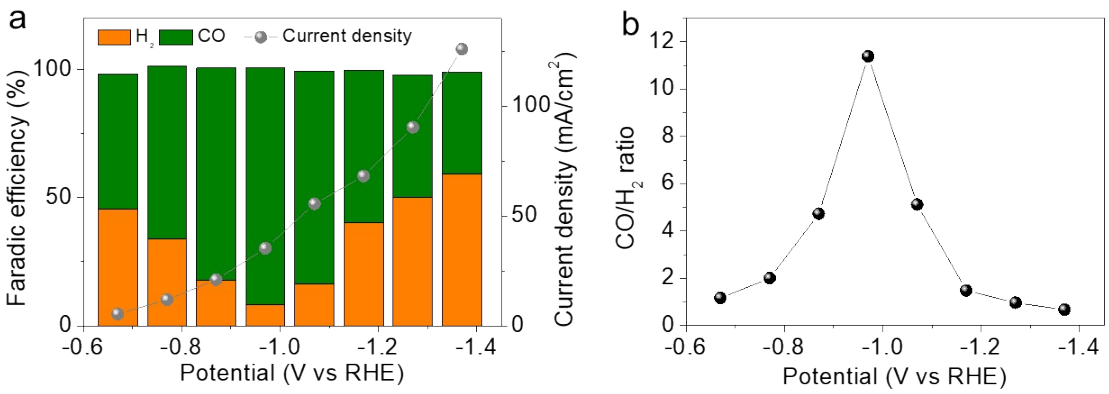


**Figure S12.** (a) $CO_2$RR performance and (b) $CO/H_2$ ratio over Zn-1P in the potential range from -0.67 V to -1.37 V vs. RHE.

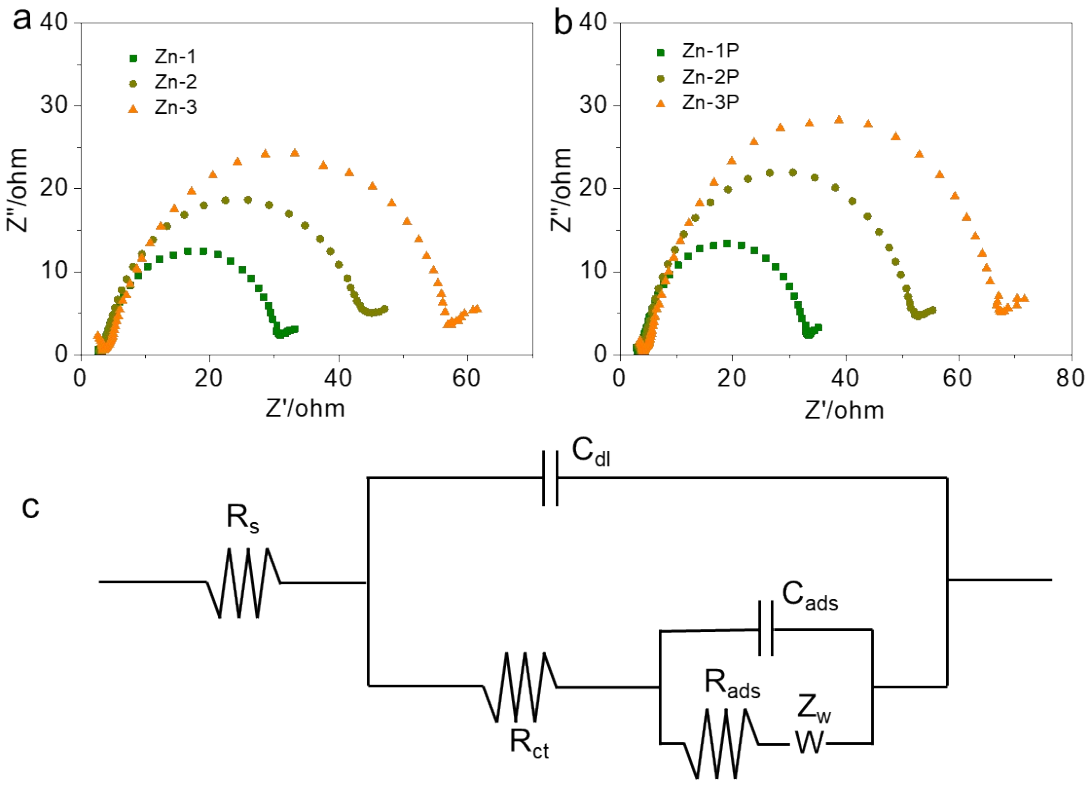


**Figure S13.** Electrochemical impedance spectroscopy of Zn-1, Zn-2, and Zn-3 (a) before and (b) after 0.3 wt.% PTFE modification. (c) Randles' equivalent circuit used for fitting the experimental impedance data. $R_s$, $R_{ct}$, $C_{dl}$, $C_{ads}$, $R_{ads}$, and $Z_w$ stand for the solution resistance, charge transfer resistance, double-layer capacitance, surface adsorption capacitance, surface adsorption resistance, and Warburg-type impedance, respectively.

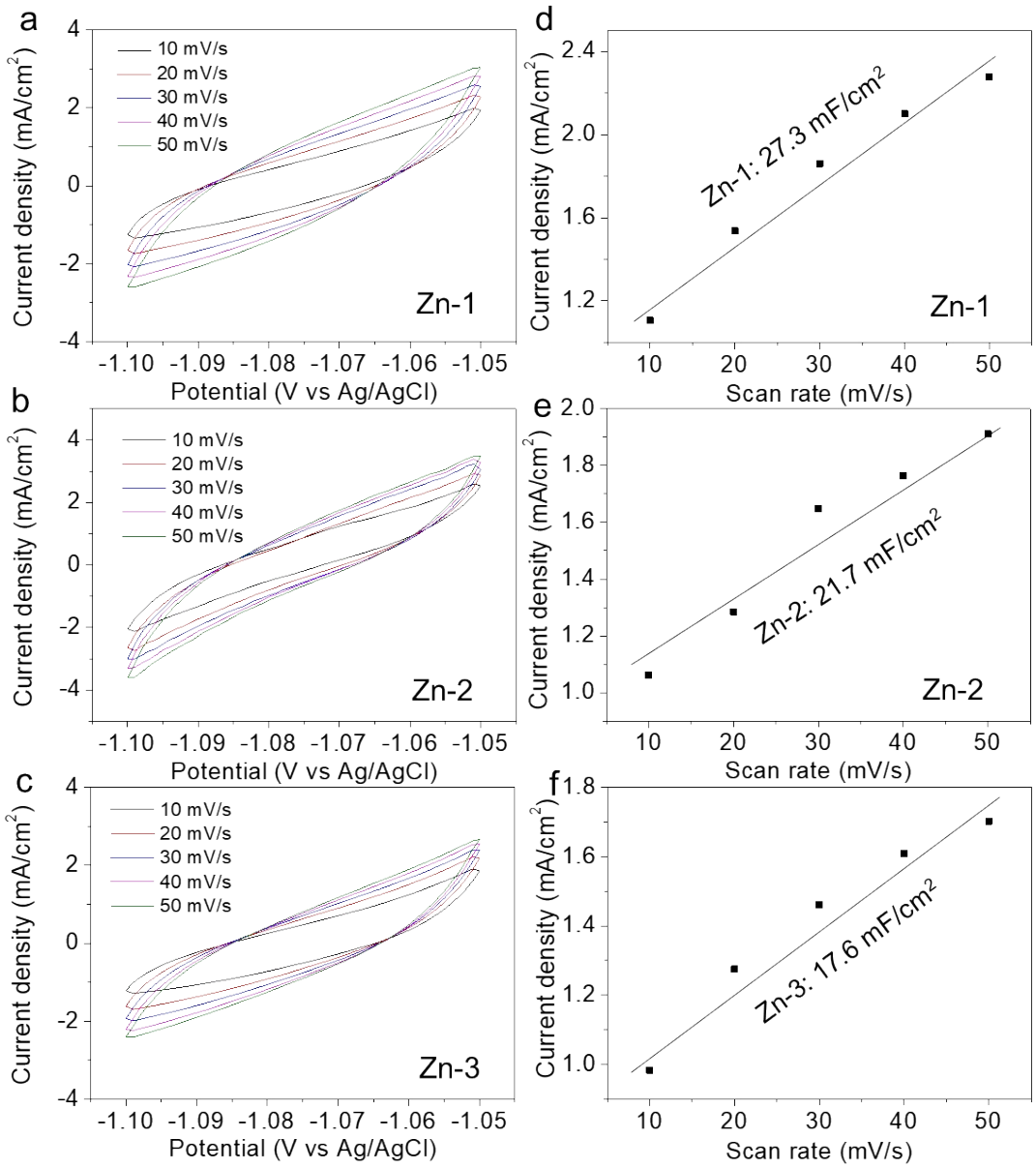


**Figure S14.** (a, b, c) Electric double layer capacitance ($C_{dl}$) measurements at the non-Faradic region (from -1.05 to -1.1 V vs. Ag/AgCl) in 0.5 M $KHCO_3$ electrolyte with saturated $CO_2$ and (d, e, f) charging current density differences Δj plotted against scan rates over Zn-1, Zn-2, and Zn-3, respectively. The slopes ($2C_{dl}$) were used to represent electrochemical active surface area (ECSA).

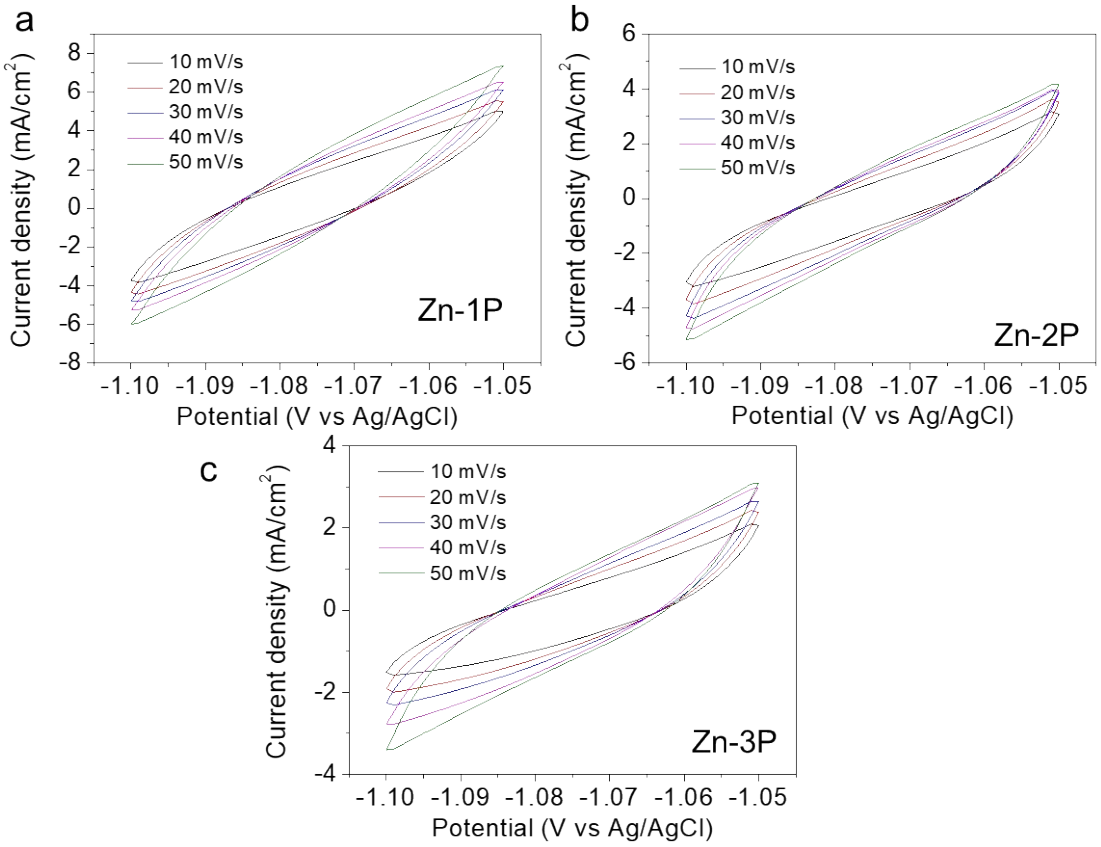


**Figure S15.** Electric double layer capacitance ($C_{dl}$) measurements at the non-Faradic region (from -1.05 to -1.1 V vs. Ag/AgCl) in 0.5 M $KHCO_3$ electrolyte with saturated $CO_2$ over (a) Zn-1P, (b) Zn-2P, and (c) Zn-3P.

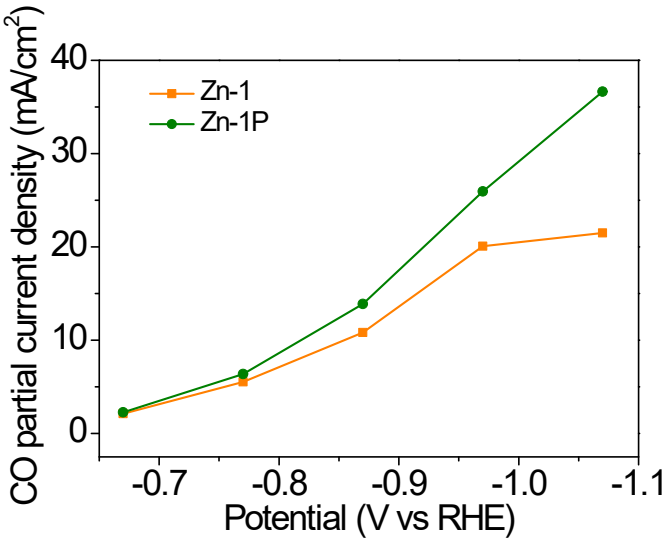


**Figure S16.** ECSA corrected CO partial current density of Zn-1 before and after 0.3 wt.% PTFE modification.

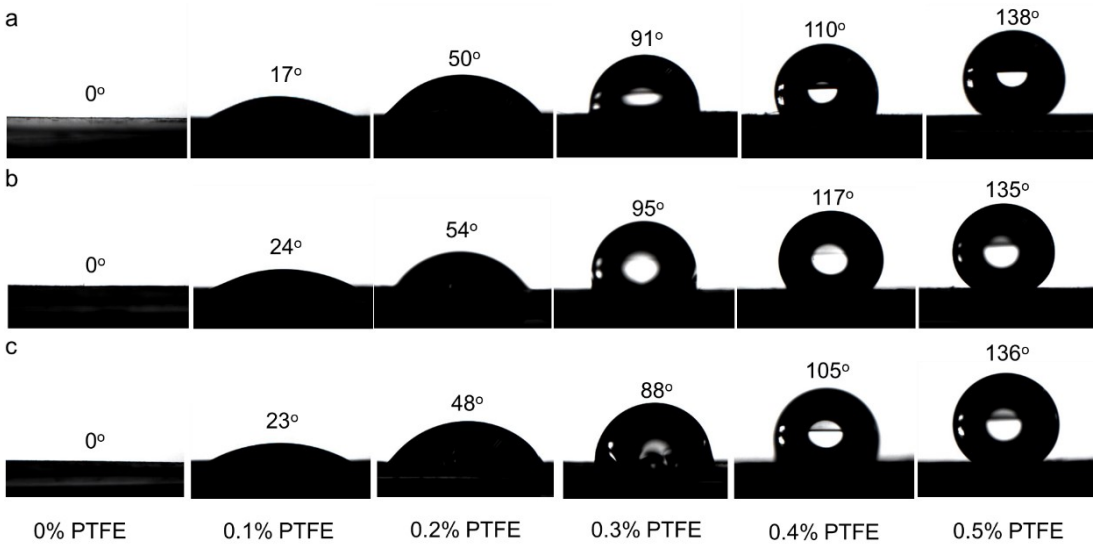


**Figure S17.** Contact angle of water on PTFE modified (a) Zn-1, (b) Zn-2 and (c) Zn-3 electrodes.

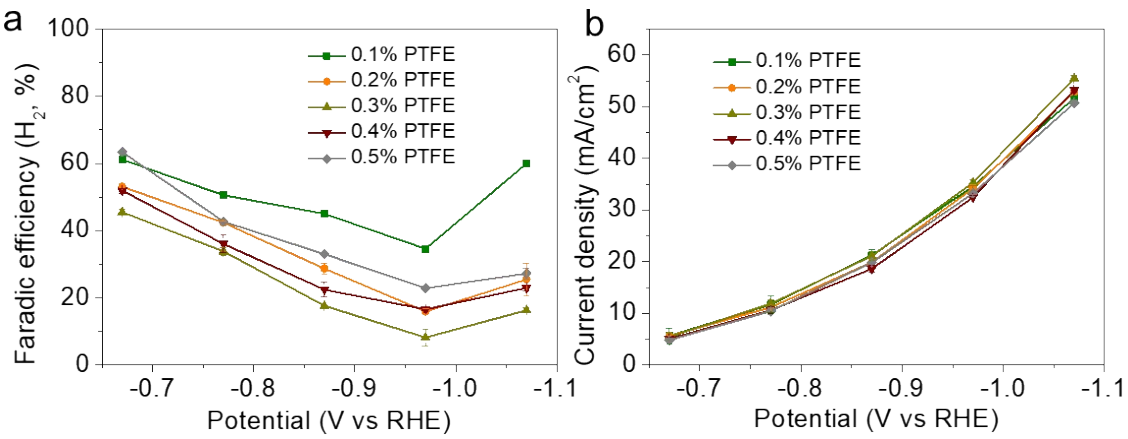


**Figure S18.** (a) $H_2$ product (b) current density of Zn-1 electrode with different amounts of PTFE modification.

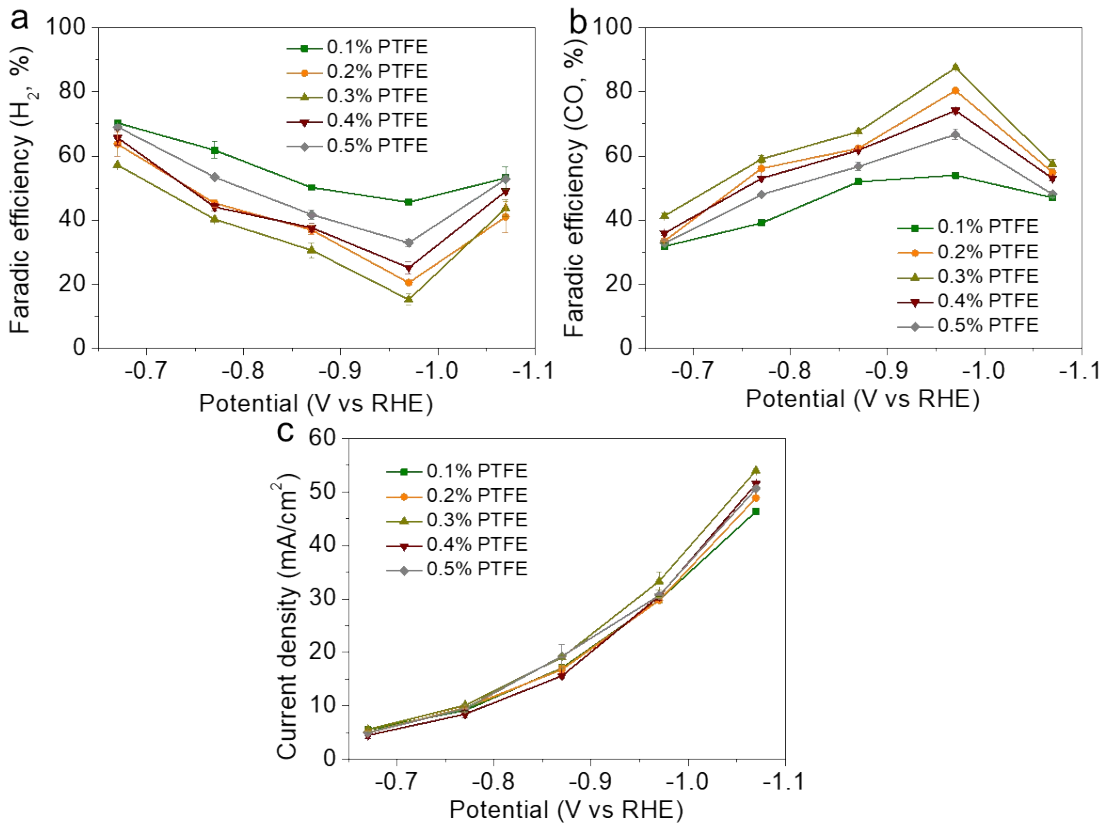


**Figure S19.** (a) $H_2$, (b) CO products, and (c) current density of Zn-2 electrode with different amounts of PTFE modification.

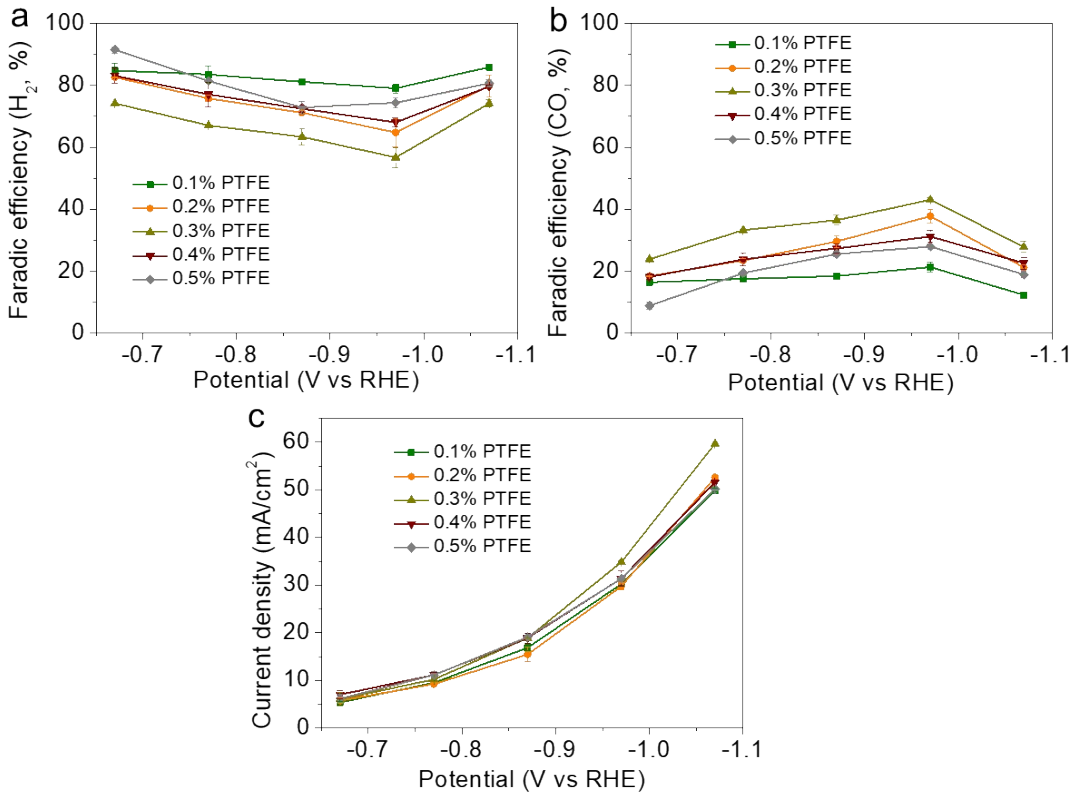


**Figure S20.** (a) $H_2$, (b) CO products, and (c) current density of Zn-3 electrode with different amounts of PTFE modification.

**Table S1.** Comparison of electrocatalytic performance with recently reported literatures for syngas production in aqueous solution.

| Catalyst | Electrolyte | Potential( V vs. RHE) | Current density ($mA/cm^2$) | $CO/H_2$ ratio | Ref. |
|---|---|---|---|---|---|
| Zn-1P | 0.5M $KHCO_3$ | -0.97 V | 35.3 | 0.09-11.4 | This work |
| Ni/FeNC | 0.5M $KHCO_3$ | -0.8 V | 27.5 | 0.33-4 | S1 |
| NiFe-NC | 0.5M $KHCO_3$ | -1.06 V | 32.58 | 0.14-10.9 | S2 |
| Ni NC/NP | 0.5M $KHCO_3$ | -0.65 V | 26 | 0.11-19 | S3 |
| ZnO | 0.1M $KHCO_3$ | -1.4 V | 23.4 | 0.28-2.11 | S4 |
| P-Au | 0.5 M $KHCO_3$ | -0.62 V | 12.5 | 0.12-0.56 | S5 |
| Ni@NCNTs | 0.5 M $KHCO_3$ | -0.8 V | 25 | 0.25-5 | S6 |
| Au/TiNS | 0.5 M $KHCO_3$ | -0.75 V | 12.2 | 0.03-4 | S7 |
| Zn | 0.1M $KHCO_3$ | -0.9 V | 11.36 | 0.2-2.31 | S8 |
| PcCu-$O_8$-Zn/CNT | 0.1M $KHCO_3$ | -0.7 V | 4 | 0.14-4 | S9 |
| CoNi-NC | 0.5 M $KHCO_3$ | -0.8 V | 37 | 0.23-2.26 | S10 |
| CuAg | 0.1M $KHCO_3$ | -0.9 V | 10 | 0.3-2 | S11 |
| AuCu | 0.1M $KHCO_3$ | -0.9 V | 11 | 0.33-4 | S12 |

## Reference


S1. X. Yang, T. Tat, A. Libanori, J. Cheng, X. Xuan, N. Liu, X. Yang, J. Zhou, A. Nashalian and J. Chen, *Materials Today*, 2021, **45**, 54-61.

S2. M. Zhang, Z. Hu, L. Gu, Q. Zhang, L. Zhang, Q. Song, W. Zhou and S. Hu, *Nano Research*, 2020, **13**, 3206-3211.

S3. W. Zhu, J. Fu, J. Liu, Y. Chen, X. Li, K. Huang, Y. Cai, Y. He, Y. Zhou, D. Su, J.-J. Zhu and Y. Lin, *Applied Catalysis B: Environmental*, 2020, **264**, 118502.

S4. B. Qin, Q. Zhang, Y.-H. Li, G. Yang and F. Peng, *ACS Applied Materials & Interfaces*, 2020, **12**, 30466-30473.

S5. L. Mascaretti, A. Niorettini, B. R. Bricchi, M. Ghidelli, A. Naldoni, S. Caramori, A. Li Bassi and S. Berardi, *ACS Applied Energy Materials*, 2020, **3**, 4658-4668.

S6. S. Shen, C. Han, B. Wang, Y. Du and Y. Wang, *Applied Catalysis B: Environmental*, 2020, **279**, 119380.

S7. F. Marques Mota, D. L. T. Nguyen, J.-E. Lee, H. Piao, J.-H. Choy, Y. J. Hwang and D. H. Kim, *ACS Catalysis*, 2018, **8**, 4364-4374.

S8. B. Qin, Y. Li, H. Fu, H. Wang, S. Chen, Z. Liu and F. Peng, *ACS Applied Materials & Interfaces*, 2018, **10**, 20530-20539.

S9. H. Zhong, M. Ghorbani-Asl, K. H. Ly, J. Zhang, J. Ge, M. Wang, Z. Liao, D. Makarov, E. Zschech, E. Brunner, I. M. Weidinger, J. Zhang, A. V. Krasheninnikov, S. Kaskel, R. Dong and X. Feng, *Nature Communications*, 2020, **11**, 1409.

S10. Q. He, D. Liu, J. H. Lee, Y. Liu, Z. Xie, S. Hwang, S. Kattel, L. Song and J. G. Chen, *Angewandte Chemie International Edition*, 2020, **59**, 3033-3037.

S11. W.-Y. Yan, C. Zhang and L. Liu, *ACS Applied Materials & Interfaces*, 2021, **13**, 45385-45393.

S12. Y. Han, Z. Wang, X. Han, W. Fang, Y. Zhou, K. Lei, B. You, H. S. Park and B. Y. Xia, *ACS Sustainable Chemistry & Engineering*, 2021, **9**, 2609-2615.